Front. Optoelectron. 2013, 6(1): 67–77
DOI 10.1007/s12200-012-0297-3

REVIEW ARTICLE

Review on SOA-MZI-based photonic add/drop and switching operations

Claudio PORZI[1], Giovanni SERAFINO[1], Sergio PINNA[1], An NGUYEN[2], Giampiero CONTESTABILE[1], Antonella BOGONI (✉)[3]

1 The TeCIP Institute of Scuola Superiore Sant'Anna di Pisa, via G. Moruzzi 1, 56124 Pisa, Italy
2 Centre d'optique, photonique et laser, 2375 rue de la Terrasse, local 2104, Université Laval, Québec, G1V 0A6, Canada
3 CNIT, via G. Moruzzi 1, 56124 Pisa, Italy

Abstract Semiconductor optical amplifier-Mach-Zehnder interferometer (SOA-MZI) is a technologically mature optical device that can be exploited for a wide range of operations on both amplitude and phase modulated signals, with performance limited by the carrier lifetime in the SOAs. Recent advances on SOA structures have demonstrated their suitability for high quality, ultra-fast photonic signal processing, making SOA-MZI a good candidate for elaborating signals in new generation high-capacity optical networks. Dynamic wavelength switching/routing and add/drop operations are expected to bring benefits in future optical networks in terms of improved system flexibility and efficiency. The capability of performing such operations directly in the optical domain can significantly reduce the number of opto/electrical and electro/optical conversions in the routing nodes, reducing their power consumption and their latency time. Moreover, since phase-shift keying (PSK) formats or other advanced modulation formats involving both amplitude and phase modulation, start to coexist in optical communication systems with the conventional on-off keying (OOK) modulation format, the availability of a single device, suitable for processing all these different signals, is mandatory. The SOA-MZI fits all these requirements for both OOK and constant-envelope phase-modulated signals, providing a compact and flexible solution. Here we review on the use of the SOA-MZI for carrying out all-optical switching operations, by realizing wavelength conversion and add/drop functionalities, both for OOK and differential binary phase shift keying (DPSK) signals up to 40 Gb/s. Power penalties lower than 2 dB are demonstrated in all cases.

Received November 8, 2012; accepted November 27, 2012

E-mail: antonella.bogoni@cnit.it

Keywords all-optical signal processing, wavelength conversion, semiconductor optical amplifier-Mach-Zehnder interferometer (SOA-MZI)

1 Introduction

Next-generation optical networks are expected to improve capacity and flexibility by dynamic wavelength switching/routing operation due to the more efficient optimization of the network resources [1,2]. The ability to perform such operation directly in optical domain can significantly reduce the number of opto/electrical and electro/optical conversions in the routing nodes. Therefore, it is very attractive in terms of latency reducing, data rate and modulation formats transparency, and potentially low-power operation thanks to photonic integration. These features become even more appealing as the transceiver complexity increases when advanced modulation formats are deployed in the transmission systems. Indeed, besides on-off keying (OOK) modulation format, pure phase and other advanced formats involving phase modulation start to play a major role in optical communication systems thanks to their higher robustness to transmission impairments [3] and to the emerging of coherent systems. For this reason, novel schemes that allow all-optical processing of phase signals can provide useful advanced functionalities in the development of all-optical network scenario. Particularly, in wavelength division multiplexed (WDM) networks, efficient wavelength conversion would provide an essential functionality for releasing a data stream at a specific wavelength from a network resource, and make the original wavelength available for new data. The wavelength converted data then can be conveniently routed onto a different wavelength path. Two separate devices would be normally required for this add/drop operation in order to

release the output fiber from the original input wavelength (space deflection) and transfer the signal information to a new output wavelength (wavelength conversion).

Many different all-optical systems implementing ultra-fast switching and/or wavelength conversion operations have been demonstrated in the past several years. These schemes exploited nonlinear phenomena taking places in semiconductor optical amplifiers (SOAs) [4–7], highly nonlinear fibers (HNLF) [8–10] or periodically-poled lithium niobate (PPLN) waveguides [11,12]. The main drawback of HNLFs is that they cannot be integrated by any means. PPLNs, on the other hand, are suitable only for hybrid integration, and have some constraints on their optical bandwidth. Furthermore, their quasi-phase matching band changes its central frequency with the working temperature; hence PPLN needs a constant temperature control. SOA is a highly non-linear optical device, which has been largely studied and exploited in the last decades. Like PPLN, SOA needs temperature stability, but it presents some advantages: it has a very large bandwidth, regardless of the temperature, and can be easily integrated; its only main limitation is switching speed, but recent works demonstrated that quantum dot (QD)-SOAs are suitable for all-optical, ultra-fast signal processing [13].

The SOA in Mach-Zehnder configuration has been proven to be a high versatile device for all-optical signal processing applications, and able to implement several functional blocks which are expected to boost the development of next-generation transparent optical networks. In recent years, the SOA-Mach-Zehnder interferometer (SOA-MZI) has been exploited for realizing a number of different operations with various modulation formats in a broad range of applications including: space switches [14], wavelength conversion [15–18], all-optical regeneration [19–23], and logical operations [24–26]. The ability to perform such a large number of operations makes the SOA-MZI a valuable tool for the development of future transparent, flexible optical communications systems in which the routing core elements will be operated more and more at purely photonic level. Able to operate as burst/packet router, ultra-fast high-performance all-optical switches and wavelength converters based on SOA-MZI can be conveniently exploited as in several noteworthy experiments reported. Up to now, however, SOA-MZIs have been usually employed in combination with other devices implementing add/drop functionalities. For instance, some SOA-MZIs have been employed as mere wavelength converters, integrated in a larger structure to perform label-based optical burst switching in general multi-protocol label switched (GMPLS) networks [27]; in another case, five SOA-MZIs have been combined to form a unique structure for signal regeneration, wavelength conversion and 40∶10 Gb/s demultiplexing [28]. A SOA-MZI has been also used in a two-section hybrid multi-granular switch comprising a micro-electro-mechanical systems (MEMS)-based switch and a SOA-MZI based switch [29], but the latter had a switching time of 1 ns, too long compared to the bit duration of typical employed bit rates.

In this article, we review an advanced scheme based on a single multi-quantum well (MQW) SOA-MZI photonic circuit, which is capable of simultaneously performing selective space deflection and wavelength conversion of a burst of data in presence of an optical gate control signal. Experiments with OOK and differential binary phase shift keying (DPSK) signals at 10 and 40 Gb/s have been carried out without any bit loss at the switched burst boundaries for both cases. The scheme operates entirely in the optical domain, thus enabling ultra-fast dynamic add/drop operation for WDM systems and packet-switched networks. By performing simultaneously the two different operations in a single step, namely data erasing and wavelength conversion at photonic level, the scheme allows to reduce the overall latency of the switch, and to minimize the number of active elements. Furthermore, the performances of the node can potentially be increased by avoiding the penalties introduced by two cascaded switches. In addition, the SOA-MZI architecture offers the possibility of handling different modulation formats; it is bit-rate transparent and thanks to the SOA broad gain spectrum, widely tunable in wavelength.

2 Operating principle for OOK signals

The device operation can be generally described as a selective wavelength shifter as depicted in Fig. 1. In the absence of any control signal, input data at λ_{in} are normally let through without wavelength conversion. Whereas, when an optical control gate is applied, they are transferred at a new wavelength λ_{new}. Thus, selective wavelength shifting of the input data depending on the control signal state is performed. However, in practical implementation, the original data without the dropped burst and the wavelength-converted data burst are available at two different fibers, which would be desirable in some practical cases. Clearly, by recollecting the two output fibers, the selective wavelength shifting operation schematically depicted in Fig. 1, is obtained.

The scheme for the implementation of the selective wavelength shifter for OOK signals is shown in Fig. 2. As illustrated in the figure, a data signal at wavelength λ_{data}, comprising a continuous wave (CW) stream of OOK modulated bits, is split into two paths and synchronously

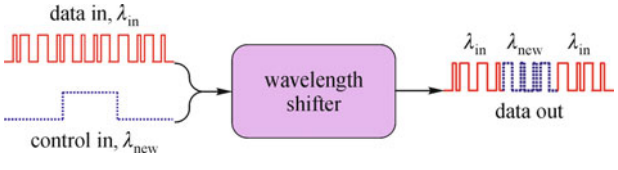

Fig. 1 Generic operation of wavelength shifter

applied to two ports IN 1 and P 1 of a SOA-MZI. In particular, the IN 1 port is a common port for the two SOAs in the interferometer arms, whereas the signal entering the P 1 port, only enters SOA 1 in the upper branch. The power levels of two replica of the data signal are independently adjusted such that the weakest replica, which acts as data probe in the device, is applied to the common port IN 1, whereas the stronger one, the data pump, is applied to the control port P 1. Similarly, a gate signal at wavelength λ_{gate} is generated and simultaneously applied to the IN 2, P 2 and P 3 ports of the SOA-MZI. In particular, the gate signal entering port IN 2 acts as a probe signal, whereas the copies entering ports P 2 and P 3 act as pump signals solely in SOA 1 and SOA 2, respectively. The input gate replicas entering ports IN 2 (the gate probe) and P 2 (gate pump 1) are synchronized in the SOA-MZI so that they crosses SOA 2 at the same time, whereas the gate signal entering port P 3 (gate pump 2) is slightly delayed with respect to gate pump 1, and its power level is lower than that of gate pump 1. Finally, a CW holding beam at wavelength λ_{HB}, is coupled together with the data probe signal to enters port IN, in order to speed up the response time of both SOA 1 and SOA 2 [30].

The operation principle can be explained as follows. By acting on the phase shifters (PSs) placed in the interferometer arms and on the SOA currents, the device is initially biased so that, in absence of any pump signal, the probe data would experience destructive interference at OUT 1. In normal operation, however, the data probe and data pump signals are always simultaneously applied to the SOA-MZI. In this way, when the gate pumps are switched off, a phase shift in the upper arm of the interferometer is produced by the marks in the data pump as effect of carrier depletion in SOA 1. The power level of the data pump signal can then be chosen such that the induced phase shift in SOA 1 cases constructive interference to occur for the data probe at OUT 1. Thus, in absence of gating signals, input data are normally presented at OUT 1, where they are retrieved at the device output by means of an optical filter centered at λ_{data} (pass-through data). When the gate signal turns high, gate probe, gate pump 1, and gate pump 2 signals enter the device from their respective inputs. In particular, the power levels of gate pump 1 and gate pump 2 are such to restore the original gain/phase balance between the two interferometer arms set by the initial bias condition. The weaker delayed gate pump 2 plays an important role for 40 Gb/s applications, since it cancels out the slow part of the phase transient induced by the onset/release of gate pump 1 in SOA 2, as explained in Ref. [15]. In this way, sharp-edged selective cancellation of the data signal at OUT 1 is obtained, which is required for operation with high data rates. It should be noted that the gate pump 2 signal is thus typically not required for operation at 10 Gb/s [31,32]. The gate pump 2 signal could be also avoided for higher data rates if faster SOAs, optimized for high-speed operation were employed in the SOA-MZI [18]. Because of the device symmetry, the initial bias settings of the device are such that the gate probe signal entering from IN 2 would also experience total destructive interference at OUT 2 if no pump signal were applied. This condition is broken by the gate pump 1 and the gate pump 2 signals that make gate probe light at λ_{gate} to appear at OUT 2. However, with a proper choice of the data pump power level, the initial condition of destructive interference at OUT 2 for the gate probe light entering from IN 2 can be restored again by the marks in the data pump signal. This results in transferring the input data pattern onto the gate signal at OUT 2 with inverted logic. An optical band-pass filter, tuned at λ_{gate} at OUT 2 can thus be used to select this inverted replica of the gated data (the wavelength-shifted signal). Clearly, the wavelength-shifted signal is presented at OUT 2 only when the original signal data are suppressed at OUT 1.

The working principle of the scheme is also illustrated in Fig. 3. Here, the normalized transmission characteristics of the SOA-MZI relating the power at OUT 1 and OUT 2 to the power at IN 1 and IN 2, respectively, are reported as a function of the phase difference $\Delta\phi$ between the interferometer's arms for the case of a perfectly balanced device. In the figure we assume, for sake of simplicity, that

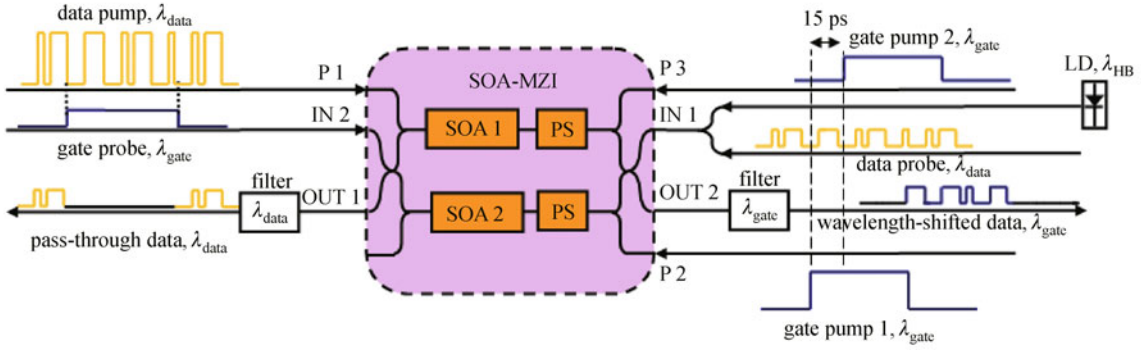

Fig. 2 Operation principle of improved scheme for 40 Gb/s OOK operations

the shape of the output/input power characteristic does not change with applied power (i.e., only a phase shift is induced in the SOAs by the pumps). We also neglect the effect of gate pump 2, as it only affects the operation of the device during the transients [15]. At OUT 1 (OUT 2), the effect of data (gate) pump is then to push the working point for the data (gate) probe from the initial low-transmission point A (A′), to the high-transmission point B (B′), so that data (gate) are output from OUT 1 (OUT 2). On the other hand, the gate (data) pump pulls back the data (gate) probe to the low-transmission point A (A′), so that data (gate) probe is cancelled in correspondence of the gate (data) pump signal. This, at the same time, cancels data in correspondence of the gate, and creates an inverted copy of the data at the gate probe wavelength.

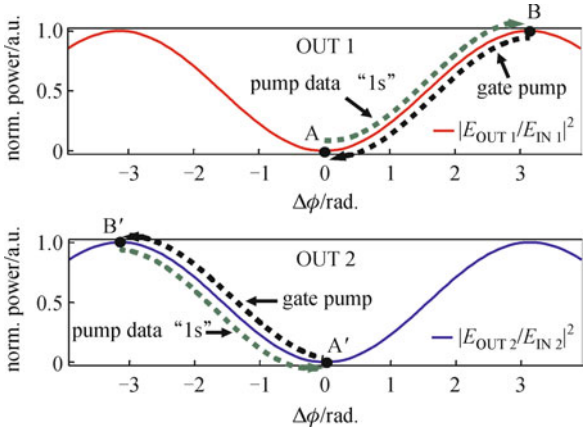

Fig. 3 Graphical description of operation, illustrating effect of pump signals on switched probes

The switching time of the interferometer structure is affected by the dynamics of the two SOAs. The gain recovery of the SOAs has been characterized, to be about 80 ps (Fig. 4(a)). The corresponding phase dynamics are then expected to operate on the same scale. This value is suitable for 10 Gb/s operation without bit loss, but at 40 Gb/s, being the recovery time longer than the bit time, it can affect the signal introducing unwanted pattern effects. This can be counteracted by using an additional holding beam. The role of the holding beam at λ_{HB}, which is injected together with the input signal with a proper power level, is to reduce the effective carrier lifetime in the SOAs, decreasing in this way the gain recovery time of the two SOAs [30]. Clearly, also the 10 Gb/s wavelength-converted data benefit by the presence of the assist light. Figure 4 also shows the different behavior of the wavelength conversion operation, with and without the holding beam for a bit rate of 10 Gb/s. In particular, Fig. 4 (b) reports the eye diagram of the output wavelength-converted signal in absence of the holding beam, whereas Fig. 4(c) shows the same signal in the presence of the holding beam. As shown by the traces, the eye opening is sensibly increased in presence of the holding beam, due to a steeper rising front with respect to the case in which the holding beam is turned off. Furthermore, for obtaining proper operation at 40 Gb/s without any bit loss, the second gate pump, as already anticipated, has also been required. This two-pump push-pull configuration, in which the gate pump 2 is properly delayed and attenuated with respect to pump 1, speeds up the interferometer response [15], thus providing sharpen transients of the switched bursts. In this way, data loss can be avoided even at data rates exceeding the intrinsic response of carriers' density restoration in the SOAs.

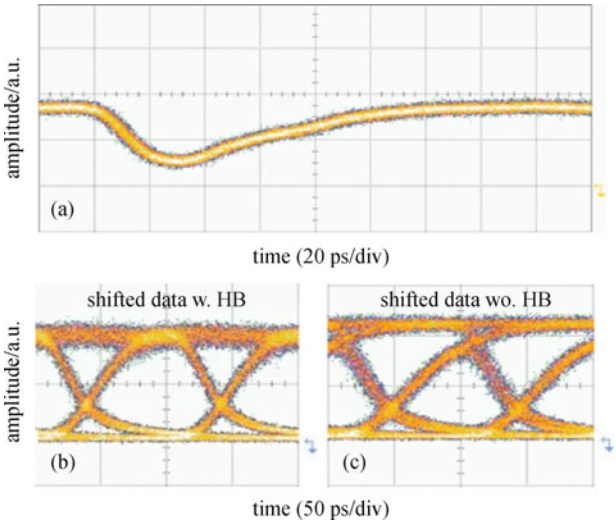

Fig. 4 Gain recovery dynamics of SOAs. (a) Gain recovery time; (b) eye diagram of wavelength-shifted output data without holding beam; (c) eye diagram of wavelength-shifted output data with holding beam

3 Experimental results with OOK signals

To demonstrate the scheme operation, we generated in two separate experiments: a 10 and 40 Gb/s non return to zero (NRZ) continuous stream of OOK data by driving a Mach-Zehnder intensity modulator (MZ-IM) with a pseudo-random-bit-sequence (PRBS) provided by a pattern generator. A squared gate/control signal with variable length was also produced using a waveform generator and a MZ-IM. In the case of 10 Gb/s data rate, the rising and falling time of the gating signal edges were measured to be about 35 ps, whereas at 40 Gb/s data rate, rising and falling time of about 10 ps for the gate signal have been obtained by employing a 40 GHz bandwidth MZ-IM. Signal wavelengths were λ_{data} = 1554 nm and λ_{gate} = 1557 nm for the data and control signal, respectively. Both signals were split to generate the various probes and pump replicas, as described before. Each probe and pump signal was synchronized at the respective SOA-MZI input ports

by means of optical delay lines. As previously explained, in the 40 Gb/s case, two gate pump signals have been employed simultaneously to speed-up the switching time of the device. In particular, the gate pump 2 signal entered port P 3 of the SOA-MZI with about 15 ps of delay with respect to the input time of gate pump 1 at port P 2 [33]. The oscilloscope traces of the input/output signals for the case of data at 10 and 40 Gb/s are shown in Figs. 4 and 5, respectively.

In the case of 10 Gb/s data, a 400 ns long gate signal with 40% duty-cycle has been used. For proper operation, the two SOAs in the interferometer arms were symmetrically driven and the pump powers were chosen to induce the proper amount of phase modulation in the two interferometer arms. The corresponding average input power levels at the SOA-MZI were −6, 0, −4.5 and 4 dBm for data probe, data pump, gate probe and gate pump, respectively, whereas the holding beam power level is set to 3 dBm. The two SOAs in the MZI were equally biased with a current of 300 mA.

For the 10 Gb/s experiment, Figs. 5(a) and 5(b) show the input data and control signals, respectively. The pass-through signal from port OUT 1 at λ_{data} is shown in Fig. 5 (d), whereas the wavelength converted signal at λ_{gate} at OUT 2 is depicted in Fig. 5(c). Details of the rising and falling edges of both output signals in switching operation are reported in Figs. 5(e) and 5(f). Rising and falling times of the shifted signal and falling time of the pass-through signal are set by the transient times of the control gate, which are close to the transients of the input data (about 35 ps, as measured on a 40 GHz sampling oscilloscope), whereas the rising time of the pass-through data are related to the carrier recovery time in SOA 1 when only the holding beam is present in the amplifier. As can be observed in Figs. 5(e) and 5(f), these dynamics do not affect noticeably the eye opening of the boundary bits. It is worth noting that a good extinction ratio of the data in the pass-through and shifted signal, as well as high suppression of the pass-through signal (which was estimated to be more than 15 dB from the oscilloscope traces) when the control gate is in the ON state, can be observed. The amplified spontaneous emission (ASE) power from the SOAs at the outputs of both the pass-band band filters in absence of input gate/probe signals was measured to be below −25 dBm. This value should ensure low noise loading in the network in absence of signals at the switch output.

The results relative to the 40 Gb/s experiment are shown in Fig. 6. In this case, a squared-wave gate signal having a period of 1 ns and 40% duty-cycle has been exploited. The corresponding average input power levels at the SOA-MZI were −9.3, 0, −7, 1.5 and −4.5 dBm for data probe, data pump, control probe and control pumps 1 and 2, respectively. The holding beam was set at 3 dBm. The two SOAs in the MZI were equally biased with a current of 380 mA. In particular, Figs. 6(a) and 6(b) show the input

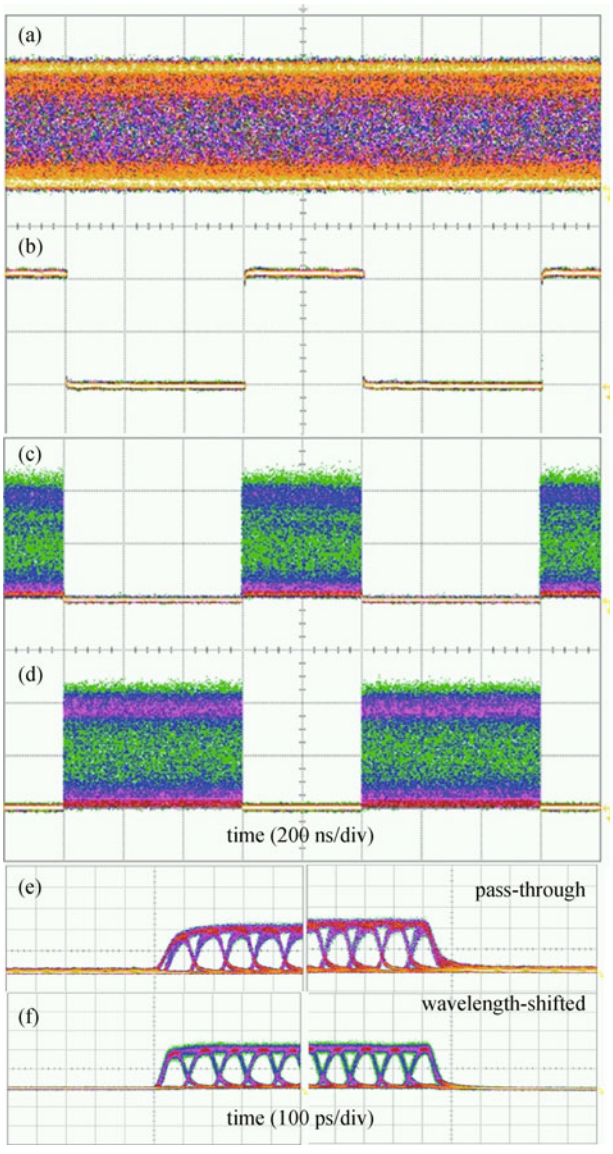

Fig. 5 Oscilloscope traces of input/output signals in the case of data at 10 Gb/s. (a) Input data; (b) gate signal; (c) wavelength-shifted output; (d) pass-through output; (e, f) transient edges of the output signals

data and gate signals, respectively. The wavelength converted signal at λ_{gate} is shown in Fig. 6(c), whereas the pass-through signal at λ_{data} is shown in Fig. 6(d). In Figs. 6(e) and 6(f), the details of the trailing and falling edges of both pass-through and wavelength-converted signals are reported. As shown, the speed-up in the phase response of the two interferometer arms, obtained by means of the push-pull configuration for the gate pump, produces a switching time shorter than bit duration, allowing in practice no bit loss for the 40 Gb/s bursts.

Results of bit error rate (BER) measurements are shown in Figs. 7 and 8 for data at 10 and 40 Gb/s respectively, relative to a $2^{11}-1$ long PRBS (limited by the gate duration that we used in the experiments). Input/output eye

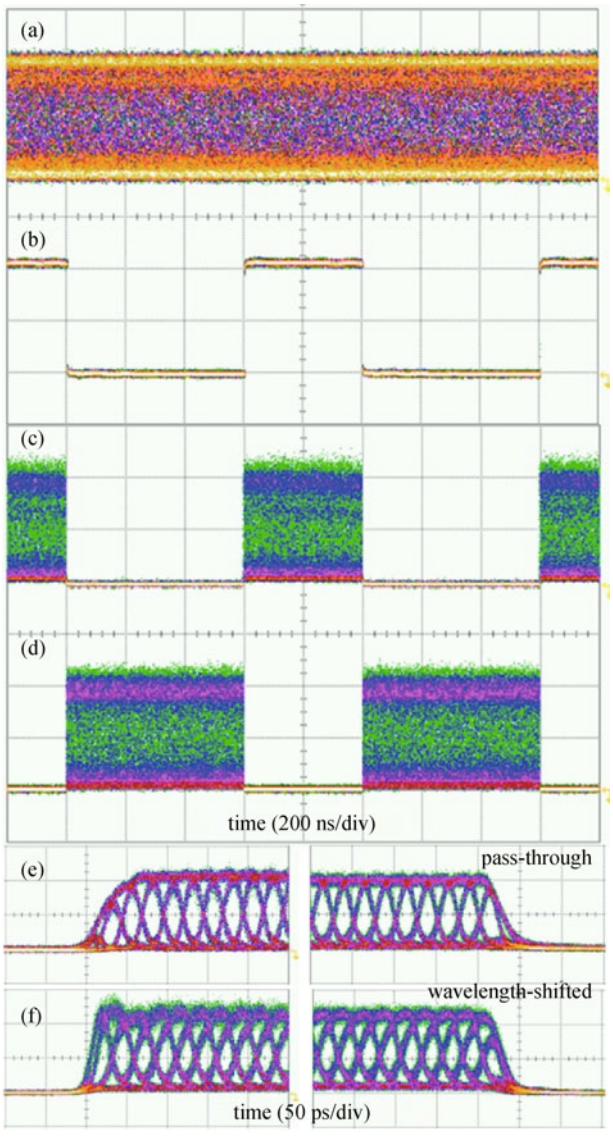

Fig. 6 Oscilloscope traces of input/output signals in the case of data at 40 Gb/s. (a) Input data; (b) gate signal; (c) pass-through output; (d) wavelength-shifted output; (e, f) transient edges of the output signals

diagrams, corresponding to error-free operation, are also illustrated in the insets of the figures. At 10 Gb/s as shown in Fig. 6, the pass-through data looks almost immune to pattern effects, due to the self-switching mechanism, which results in a negligible power penalty of about 0.2 dB (at a BER of 10^{-9}). On the other hand, the eye diagram of the wavelength converted signal shows a slower transient in its leading edge, corresponding to the falling edge of the data pump, because of carriers' dynamics in SOA 2. For this signal, a power penalty of about 0.85 dB was measured at BER = 10^{-9}. Also in the case of 40 Gb/s experiment, the eye-diagrams and bit-error rate measurements reported in

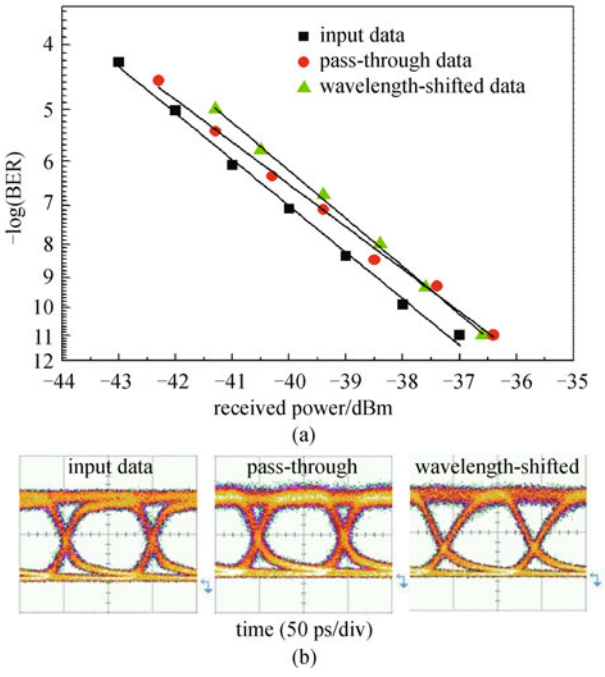

Fig. 7 BER measurements results (a) and input/output eye diagrams (b) at 10 Gb/s. The extinction ratio is 12.5, 12.1, and 11.8 dB for the input, pass-through and shifted eye diagram, respectively

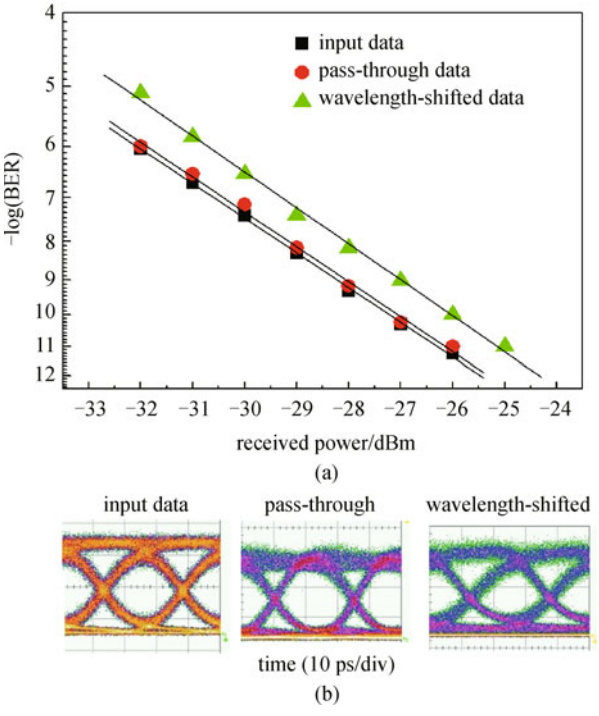

Fig. 8 BER measurements results (a) and input/output eye diagrams (b) at 40 Gb/s. The extinction ratio is 12, 11.4 and 9.8 dB for the input, pass-through and shifted eye diagram, respectively

Fig. 8, show that the pass-through data are almost unaffected by the switch, showing a negligible power penalty of about 0.3 dB. On the other side, whereas the wavelength converted signal is only slightly distorted by the wavelength conversion process, corresponding in a larger power penalty for the wavelength-converted data, which has been measured to be about 1.4 dB.

4 Operating principle for PSK signals

The proposed scheme allowing to perform simultaneous switch and wavelength conversion operation in a single SOA-MZI can be suitably modified for dynamic wavelength routing and add/drop operations of PSK signals [34]. The corresponding operation principle of the modified scheme is illustrated in Fig. 9. As shown in Fig. 9, a DPSK data signal at wavelength λ_{data} is simultaneously applied to two ports of a SOA-MZI: similarly to the previous OOK case, one replica of the input data, acting as a probe signal for both SOAs, is applied to the port IN 1 whereas the other replica, acting as a data pump solely in SOA 2, is applied to port P 1 of the device. The two SOAs inside the MZI are driven with different bias current values, so that the interferometer is initially unbalanced, and the PSs placed on the interferometer's arms are set in such a way that the data probe signal entering IN 1 would experience partial destructive interference at OUT 1, if no other signal is applied to the device. In normal operation, however, the data probe and pump signals always enter simultaneously the device. In particular, the pump power level is such to induce a phase shift in SOA 2 leading to constructive interference at OUT 1 for the probe signal, hence maximizing its transmission. Thus, in absence of the gate signal, the output data probe is normally let through OUT 1 of the device (pass-through data in the figure). When a gate signal at λ_{gate} with an appropriate power level is input to the device from IN 2, two effects occur inside the SOA-MZI. First, the gain of the two SOAs is significantly reduced with a consequent decrease of the data probe power at the output of SOA 1 and SOA 2 to approximately the same level. The second effect is an induced extra phase shift in both SOAs. However, since SOA 1 is operating in the small-signal gain regime before the gate signal enters the device, the corresponding pump-induced phase shift in SOA 1 is larger than that occurring in SOA 2, which is already operating in a partially saturated regime due to the presence of pump data. For a given suitable level of unbalance in the SOAs driving currents and of saturation in SOA 2, it is then possible to impress a π phase difference between the two data probe fields emerging from SOA 1 and SOA 2 by properly adjusting the gate signal power level. As the amplitude of the data probe fields leaving the highly saturated SOA 1 and SOA 2 is also equalized, this reflects into total destructive interference at OUT 1, leading to a strong suppression of the pass-through data probe in correspondence of the gate signal. At the same time, the gate and data pump signals nonlinearly interact inside SOA 2, giving rise to several four wave mixing (FWM) components; in particular, one of the two first-order generated FWM components is the complex conjugated replica of the data signal. This wavelength converted replica of the data signal at λ_{FWM} (wavelength-shifted data in Fig. 9) thus appears at OUT 2 port of the device only when the pass-through data are cancelled at OUT 1, and can be selected by means of a bandpass optical filter tuned at λ_{FWM}. The FWM complex conjugate operation preserves anyway the input DPSK data encoding.

Also in this case, we can explain the principle of operation by considering the SOA-MZI transfer characteristic under the different operating conditions. This is schematically illustrated in Fig. 10, where the data probe output power (at OUT 1) is plotted as a function of the phase difference in the interferometer arms, $\Delta\phi$. In the figure it is shown that, when only the data probe enters the device, the SOA-MZI is suitably biased at the point named A′. The effect of applying a data pump is a new output characteristic and a phase shift in SOA 2 that moves the working point to the point named A in the figure. This is the working point on OUT 1 power characteristic when both the data pump and probe signals are injected into the device. When the gate signal at λ_{gate} is input to the device from IN 2 with an appropriate power level, two effects

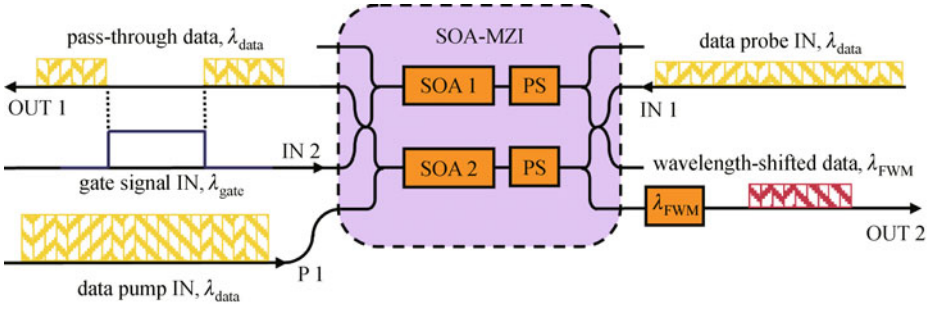

Fig. 9 Operation principle of modified proposed scheme for 40 Gb/s PSK operations

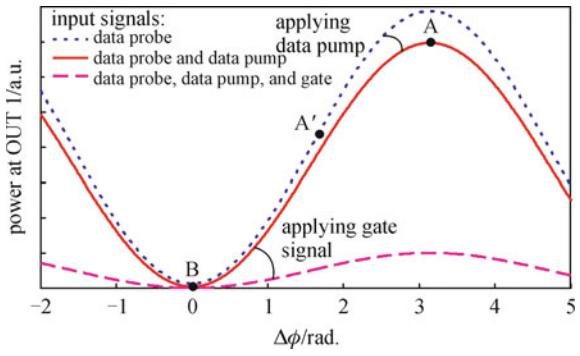

Fig. 10 Graphical description of SOA-MZI switch for pass-trough/data erasing operation

occur inside the SOA-MZI. First, the amplifiers gain is significantly reduced so that the data probe power at the output of both SOAs decreases to approximately the same level. The second effect is an induced extra phase shift in both SOAs. However, since SOA 1 is in the small-signal gain regime before the gate enters the device, the corresponding pump-induced phase shift is larger than that occurring in SOA 2, which is already partially saturated by the pump data.

5 Experimental results with PSK signals

In two separate experiments, we generated a continuous stream of 10 and 40 Gb/s DPSK modulated optical data and a gate signal. The gate signal was a 500 ns long squared signal with a duty-cycle of 50%. Data and gate wavelengths were fixed at λ_{data} = 1554.2 nm and λ_{gate} = 1552.9 nm, respectively. The data stream was split into two paths to generate the probe and pump replicas; the data probe and pump signals were then synchronized at the respective SOA-MZI inputs by means of delay lines. Driving currents of SOA 1 and SOA 2 were 380 and 420 mA, respectively. In the 10 Gb/s experiment, power levels at the SOA-MZI input ports were −4, 8 and 13 dBm for data probe, data pump, and control gate signals, respectively, whereas in the 40 Gb/s experiment power levels at the SOA-MZI input ports were −4, 10.6 and 15.7 dBm for data probe, data pump, and control gate signals, respectively.

The corresponding optical spectra at SOA 2 output are shown in Fig. 11. The FWM-generated signals at λ_{FWM} = 1551.6 nm show an output OSNR (on 0.1 nm resolution bandwidth) of around 30 dB in both cases. The oscilloscope traces of the input/output signals corresponding to the 10 and 40 Gb/s cases are shown in Fig. 12. From the top to the bottom, the input data, the control gate, the pass-through data, the wavelength-shifted data, and the transients of the demodulated switched bursts (including also the 40 Gb/s case), are reported. A complete cancellation of the data burst in the pass-through signal can be observed (more than 15 dB calculated from the oscilloscope traces) when the control gate is in the ON state. The details of the rising and falling edges of switched output signals, shown in Figs. 12(e) to 12(h), confirm that the switching dynamics are fast enough to prevent any bit loss at the boundaries after demodulation with standard 1-bit delay interferometer for both 10 and 40 Gb/s modulated data. The input/output demodulated eye diagrams, as well as BER measurements, are reported in Fig. 13 for both the 10 and 40 Gb/s experiments.

The BER of demodulated data eye diagrams was measured to be about 11 dB for all the input/output signals in both the 10 and 40 Gb/s experiments. The results of BER measurements with a $2^{11}-1$ long PRBS (limited by

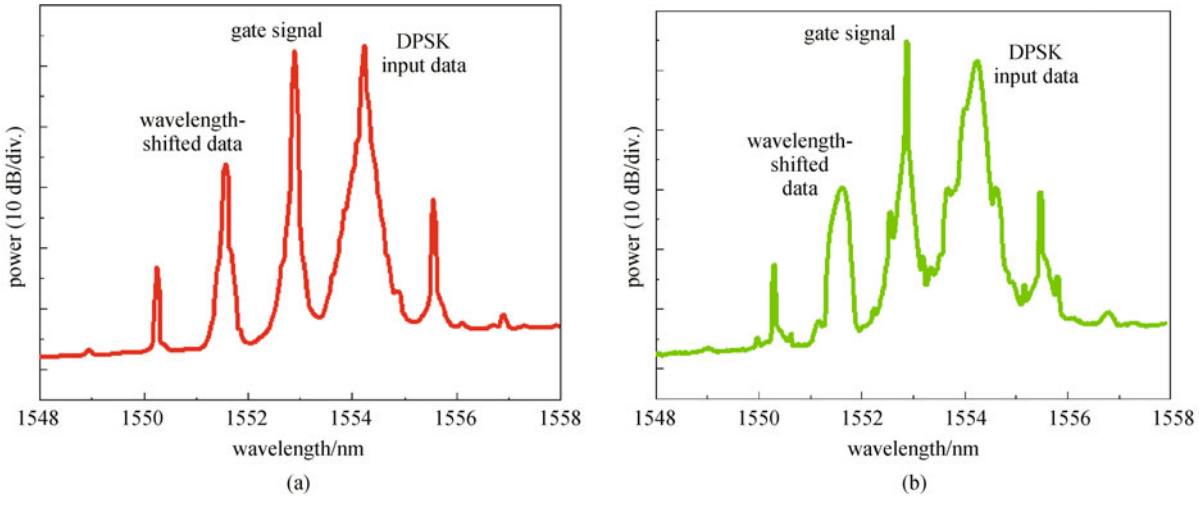

Fig. 11 Output spectra from SOA 2 with 10 (a) and 40 Gb/s (b) DPSK modulated data (res.: 0.1 nm)

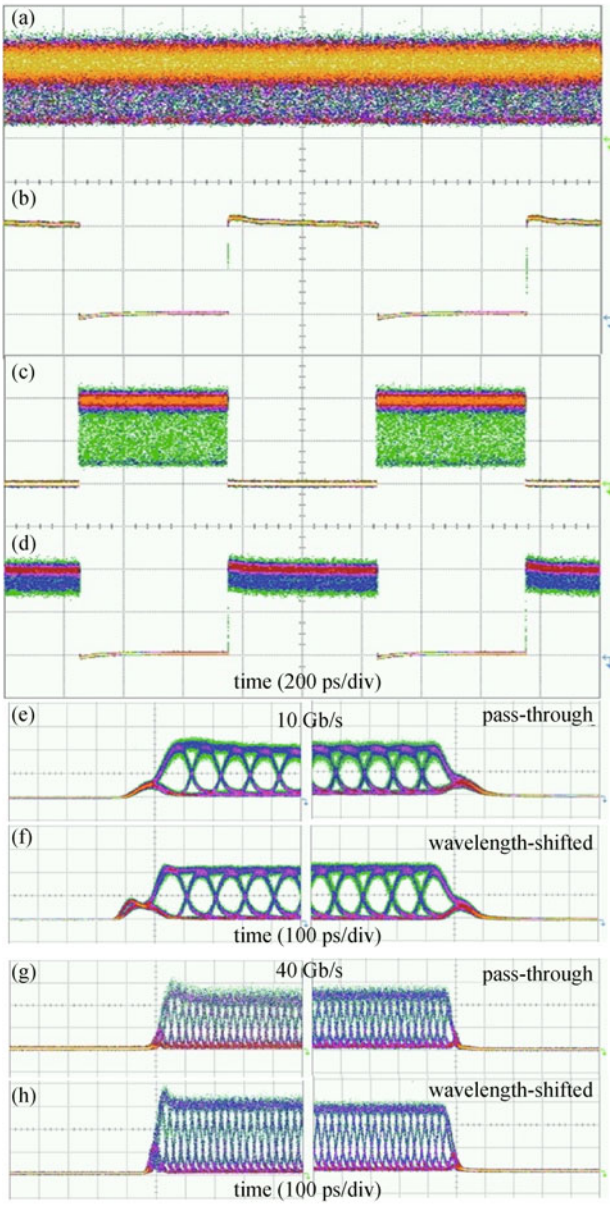

Fig. 12 Oscilloscope traces of input/output signals in the case of DPSK modulated data. (a) Input data; (b) gate signal; (c) pass-through output; (d) wavelength-shifted output; (e, f) transient edges of the output signals at 10 Gb/s; (g, h) transient edges of the output signals at 40 Gb/s

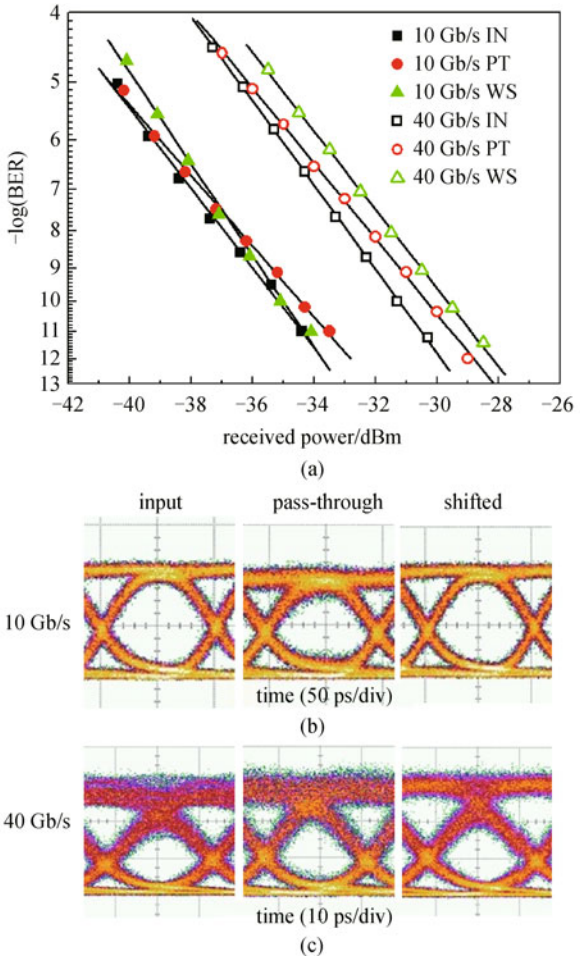

Fig. 13 (a) BER measurements for input (IN), pass-trough (PT) and wavelength-shifted (WS) data at 10 and 40 Gb/s; (b) eye diagrams of input/output demodulated data at 10 Gb/s; (c) eye diagrams of input/output demodulated data at 40 Gb/s

gate duration) confirmed the effectiveness of the proposed technique, as shown in Fig. 13. Almost negligible power penalty (at BER = 10^{-9}) with respect to the input data for both the pass-through (0.5 dB) and wavelength-shifted data (0.2 dB) was observed at 10 Gb/s, whereas a power penalty (at BER = 10^{-9}) of about 1 and 1.5 dB for the pass-through and shifted data, respectively, was observed at 40 Gb/s. By using orthogonal double-pump FWM [35], flat conversion efficiency over a fair portion of the SOA gain spectrum could be easily achieved, enabling wide-band conversion range operation. Alternatively, FWM architecture with two parallel pumps can be implemented to make the scheme operation transparent to input data wavelength and polarization [36].

6 Conclusions

We propose novel and effective methods enabling all-optical switching, by means of simultaneous data erasing and wavelength conversion of a burst of data selected by an optical gate signal. The presented scheme is suitable for high-speed dynamic wavelength routing and/or add/drop operation in WDM networks. All the solutions operate entirely in the photonic domain and are based on a single integrated SOA-MZI, which can in principle operate with OOK and any constant-envelope advanced phase-modulated signal, like M-ary PSK. The device enables wide-band conversion operation over the entire C band [32] and

it can be transparent to input data wavelength and polarization. Reduced power penalty as well as faster operation up to 40 Gb/s have been obtained.

References

1. Andriolli N, Buron J, Ruepp S, Cugini F, Valcarenghi L, Castoldi P. Label preference schemes in GMPLS controlled networks. IEEE Communications Letters, 2006, 10(12): 849–851
2. Azodolmolky S, Klinkowski M, Marin E, Careglio D, Pareta J S, Tomkos I. A survey on physical layer impairments aware routing and wavelength assignment algorithms in optical networks. Computer Networks, 2009, 53(7): 926–944
3. Gnauck A H, Winzer P J. Optical phase-shift-keyed transmission. IEEE/OSA Journal of Lightwave Technology, 2005, 23(1): 115–130
4. Schubert C, Schmidt-Langhorst C, Schulze K, Marembert V, Weber H G. Time division add-drop multiplexing up to 320 Gbit/s. In: Proceedings of Conference on Optical Fiber Communication Conference. 2005, 4, OThN2
5. Phillips D, Ellis A D, Thiele H J, Manning R J, Kelly A E. 40 Gbit/s all optical regeneration and demultiplexing using a semiconductor non-linear interferometer. IEE Electronics Letters, 1998, 34(24): 2340–2342
6. Diez S, Ludwig R, Weber H G. Gain-transparent SOA-switch for high-bitrate OTDM add/drop multiplexing. IEEE Photonics Technology Letters, 1999, 11(1): 60–62
7. Liu Y, Tangdiongga E, Li Z, Zhang S, de Waardt H, Khoe G D, Dorren H J S. Error-free all-optical wavelength conversion at 160 Gb/s using a semiconductor optical amplifier and an optical bandpass filter. IEEE/OSA Journal of Lightwave Technology, 2006, 24(1): 230–236
8. Verdurmen E J M, Zhao Y, Tangdiongga E, Turkiewicz J P, Khoe G D, de Waardt H. Error-free all-optical add-drop multiplexing using HNLF in a NOLM at 160 Gbit/s. IEE Electronics Letters, 2005, 41 (6): 340–350
9. Mulvad H, Galili M, Oxenlowe L K, Clausen A T, Jeppesen P, Gruner-Nielsen L. 640 Gbit/s optical time-division add-drop multiplexing in a non-linear optical loop mirror. IEEE/LEOS Winter Topicals Meeting Series, 2009, 209–210
10. Wadsworth W J. Nonlinear wavelength conversion and pulse manipulation in photonic crystal fibres. In: Proceedings of Eouropean Conference Optical Communication. 2010, Th.9.F.1
11. Bogoni A, Wu X, Fazal I, Willner A. 160 Gb/s time-domain channel extraction/insertion and all-optical logic operations exploiting a single PPLN waveguide. IEEE/OSA Journal of Lightwave Technology, 2009, 27(19): 4221–4227
12. Liu S, Kwang J L, Kakande J, Parmigiani F, Slavik R, Petropoulos P, Richardson D J, Gallo K. Phase-sensitive wavelength conversion based on cascaded quadratic processes in periodically poled lithium niobate waveguides. In: Proceedings of Conference on Optical Fiber Communication. 2011, Th.9.F.1.
13. Contestabile G, Maruta A, Sekiguchi S, Morito K, Sugawara M, Kitayama K. All-optical signal processing using QD-SOA. In: Proceedings of Electronics and Communications Conference. 2010, 200–201
14. Leuthold J, Besse P A, Eckner J, Gamper E, Dülk M, Melchior H. All-optical space switches with gain and principally ideal extinction ratios. IEEE Journal of Quantum Electronics, 1998, 34(4): 622–633
15. Nakamura S, Tajima K. Bit-rate-transparent non-return-to-zero all-optical wavelength conversion at up to 42 Gb/s by operating symmetric-Mach-Zehnder switch with new scheme. In: Proceedings of Conference on Optical Fiber Conference. 2004, FD3
16. Hattori M, Nishimura K, Inohara R, Usami M. Bidirectional data injection operation of hybrid integrated SOA-MZI all-optical wavelength converter. IEEE/OSA Journal of Lightwave Technology, 2007, 25(2): 512–519
17. Yi X, Yu R, Kurumida J, Ben Yoo S J. A theoretical and experimental study on modulation-format-independent wavelength conversion. IEEE/OSA Journal of Lightwave Technology, 2010, 28 (4): 587–595
18. Hatta T, Miyahara T, Miyazaki Y, Takagi K, Matsumoto K, Aoyagi T, Motoshima K, Mishina K, Maruta A, Kitayama K. Polarization-insensitive monolithic 40-Gbps SOA-MZI wavelength converter with narrow active waveguides. IEEE Journal on Selected Topics in Quantum Electronics, 2007, 13(1): 32–39
19. Poustie A, Wyatt R, McDougall R, Maxwell G, Hemenway B R. Optical timing jitter transfer characteristics of a 40 Gb/s hybrid integrated SOA-Mach-Zehnder interferometer all-optical regenerator. In: Proceedings of European Conference on Optical Communication. 2005, 3, 413–414
20. Apostolopoulos D, Simos H, Petrantonakis D, Bogris A, Spyropoulou M, Bougioukos M, Vyrsokinos K, Pleros N, Syvridis D, Avramopoulos H. A new scheme for regenerative 40 Gb/s NRZ wavelength conversion using a hybrid integrated SOA-MZI. In: Proceedings of Conference on Optical Fiber Communication. 2010, OThS6
21. Kang I, Dorrer C, Zhang L, Rasras M, Buhl L, Bhardwaj A, Cabot S, Dinu M, Liu X, Cappuzzo M, Gomez L, Wong-Foy A, Chen Y F, Patel S, Neilson D T, Jacques J, Giles C R. Regenerative all-optical wavelength conversion of 40 Gb/s DPSK signals using a SOA MZI. In: Proceedings of the 31st European Conference on Optical Communication. 2005, 6, 29–30
22. Petrantonakis D, Zakynthinos P, Apostolopoulos D, Poustie A, Maxwell G, Avramopoulos H. All-optical four-wavelength burst mode regeneration using integrated quad SOA-MZI arrays. IEEE Photonics Technology Letters, 2008, 20(23): 1953–1955
23. Wang J P, Savage S J, Robinson B S, Hamilton S A, Ippen E P, Mu R, Wang R, Spiekman L, Stefanov B B. Regeneration using an SOA-MZI in a 100-pass 10000-km recirculating fiber loop. In: Proceedings of Conference on Lasers and Electro-Optics. 2007, CMZ1
24. Kim J Y, Kang J M, Kim T Y, Han S K. All-optical multiple logic gates with XOR, NOR, OR, and NAND functions using parallel SOA-MZI structures: theory and experiment. IEEE/OSA Journal of Lightwave Technology, 2006, 24(9): 3392–3399
25. Martinez J M, Herrera J, Ramos F, Marti J. All-optical correlation employing single logic XOR gate with feedback. IEE Electronics Letters, 2006, 42(20): 1170–1171
26. Aikawa Y, Shimizu S, Uenohara H. Demonstration of all-optical divider circuit using SOA-MZI-type XOR gate and feedback loop for forward error detection. IEEE/OSA Journal of Lightwave

Technology, 2011, 29(15): 2259–2266
27. Vlachos KG, Monroy I T, Koonen A M J, Peucheret C, Jeppesen P. STOLAS: switching technologies for optically labeled signals. IEEE Communications Magazine, 2003, 41(11): 9–15
28. Pleros N, Zakynthinos P, Poustie A, Tsiokos D, Bakopoulos P, Petrantonakis D, Kanellos G.T, Maxwell G, Avramopoulos H. Optical signal processing using integrated multi-element SOA–MZI switch arrays for packet switching. IET Optoelectronics, 2007, 1(3): 120–126
29. Zervas G, Sadeghioon L, Klonidis D, Qin Y, Nejabati R, Simeonidou D. Demonstration of novel multi-granular switch architecture on an application-aware end-to-end multi-bit rate OBS network testbed. In: Proceedings of ECOC 2007 Post-deadline papers. 2007, 1–2
30. Manning R J, Davies D A O. Three-wavelength device for all-optical signal processing. Optics Letters, 1994, 19(12): 889–991
31. Nguyen A, Porzi C, Serafino G, Fresi F, Contestabile G, Bogoni A. All-optical gated wavelength converter-eraser using a single SOA-MZI. IEEE Photonics Technology Letters, 2011, 23(21): 1621–1623
32. Pinna S, Porzi C, Contestabile G, Bogoni A. Broadband operation of high-speed all-optical gated wavelength shifter. IEEE Photonics Technology Letters, 2012, 24(17): 1546–1548
33. Nguyen A, Porzi C, Pinna S, Contestabile G, Bogoni A. 40 Gb/s all-optical selective wavelength shifter. In: Proceedings of Conference on CLEO 2012: Science and Innovations. 2012, CM2A.2
34. Porzi C, Contestabile G, Bogoni A. All-optical simultaneous drop and wavelength conversion of DPSK data. Optics Letters, 2012, 37 (13): 2523–2525
35. Morgan T J, Lacey J P R, Tucker R S. Widely tunable four-wave mixing in semiconductor optical amplifiers with constant conversion efficiency. IEEE Photonics Technology Letters, 1998, 10(10): 1401–1403
36. Porzi C, Bogoni A, Potì L, Contestabile G. Polarization and wavelength-independent time-division demultiplexing based on copolarized-pumps FWM in an SOA. IEEE Photonics Technology Letters, 2005, 17(3): 633–635